



## OPTIMIZATION OF A POLYGONAL HOLLOW STRUCTURAL STEEL SECTION IN THE ELASTIC REGION

John Samuel Kabanda  
PhD candidate, Queen's University, Canada

Colin MacDougall  
Associate Professor, Queen's University, Canada







### ABSTRACT

Square, rectangular, circular, elliptical, and oval steel hollow structural sections are commonly used in a wide range of structural applications. The need for deep sections with increased bending stiffness has been the motivation for polygonal hollow structural sections. Polygonal hollow structural sections can have a higher bending strength, and rotational capacity when compared to traditional rectangular or square hollow structural sections with similar cross-sectional area. This paper discusses the numerical optimization of one such polygonal hollow structural section currently used in Canada. Previously conducted full-scale beam bending tests provide data for the calibration of the numerical model. The optimized cross-section has a 9.4% higher bending stiffness with no increase in cross-sectional area as compared to the original design. If a 19.6% increase in cross-sectional area is permitted, the optimized cross-section has a 40.5% higher bending stiffness than the original design.

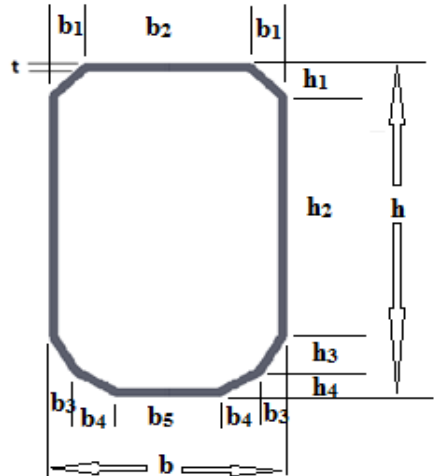
### 1. INTRODUCTION

In the construction industry and other engineering sectors, square, rectangular, circular, and other specialised steel hollow structural sections (HSS), shown in Table 1, have become more widely used due to their structural efficiency and aesthetics. The recent addition is the polygonal hollow structural section (PHSS). The advantage of the PHSS is the increase in bending strength, and rotational capacity it offers as the number of corners of its cross-section increases (Yamashita et al., 2003).

Table 1: Examples of specialized steel hollow structural sections

	triangular	hexagonal	octagonal	flat - oval	elliptical	half-elliptical
shape						

The PHSS herein starts as a basic rectangular HSS (RHSS) but includes bends in its web and flange, as shown in Figure 1, to reduce the potential for local buckling,. Another way to minimize the potential of local buckling is to use an oval HSS (OHSS). However, a disadvantage of the OHSS is that its constantly changing radius requires specialized manufacturing expertise, especially for welded sections. In contrast, the flanges of the PHSS are easier to fabricate as they require only a discrete number of plate bends rather than a continuous curvature. Furthermore, the corners of the flanges of the PHSS maintain a minimum radius of  $3t$ , where  $t$  is the wall thickness. This increases its rotational capacity, and ensures that no microscopic stress cracks and brittle-type failures occur during galvanizing.



where;  $h$  is the height,  $b$  is the width and  $t$  is the thickness of the cross-section.

Figure 1: Proposed cross-section of the PHSS beam with the different dimension variables

The PHSS shown in Figure 1 is used in cantilever applications so that compression occurs primarily in the bottom flange. The additional bends on the bottom flange maximize resistance to local buckling while minimizing weight. This does mean the PHSS is not symmetric about its horizontal axis and a reversal of loading could lead to local buckling of the top flange. In practice, however, reversal of loading rarely occurs.

However, research on PHSS beams for engineering applications is limited. In one of the most recent studies, Yamashita et al., 2003 only considered the crush behaviour of short PHSS stub-columns (200 mm long) under axial compression, and there is also a lack of proper design guidance hindering more widespread use in the industry. As a result, a full-scale experimental four-point flexural bending test program was initiated using a proposed cross-section of the PHSS beam, Figure 2.



Figure 2: Flexural bending experimental test set-up

The results showed that the proposed PHSS has a higher bending strength, and rotational capacity, Figure 3, when compared to a traditional RHSS with similar cross-sectional area.

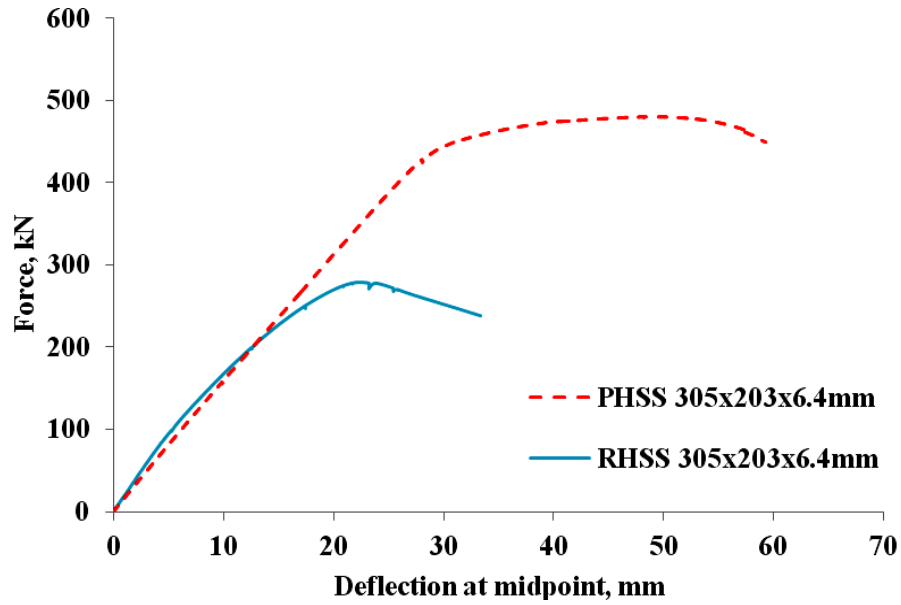


Figure 3: Applied load vs deflection comparison between PHSS and RHSS beams

Following completion of the experimental tests, a design optimization study was initiated. The purpose of this study was to further improve the bending stiffness of PHSS beams as experimental tests would be too costly for this purpose. This paper discusses the optimization analysis of the proposed cross-section of one of the PHSS beams that was used to complete the experimental flexural bending tests.

The optimization process was carried out by numerically varying the cross-sectional dimensions of the proposed cross-section of the PHSS beam with the objective function of minimizing deflection, and thus increasing stiffness. The numerical optimization and finite element analyses were completed in ANSYS Mechanical APDL 15.0. The initial dimensions of the proposed cross-section of the PHSS beam are listed in Table 2.

Table 2: Initial Dimensions of the proposed cross-section of the PHSS beam

Design Variable	Length (mm)
b	203
b <sub>1</sub>	49.5
b <sub>2</sub>	104
b <sub>3</sub>	33.5
b <sub>4</sub>	42
b <sub>5</sub>	52
h	305
h <sub>1</sub>	57
h <sub>2</sub>	191
h <sub>3</sub>	39.6
h <sub>4</sub>	17.4
t	6.4

## 2. METHODOLOGY

The purpose of this optimization study was to obtain the cross-section of the PHSS beam which maximized its bending stiffness. An optimization analysis requires an objective function, design variables, and a state variable. The objective function is the parameter being optimized. The design variables are the parameters that are varied to change the objective function, and the state variable provides a constraint or constraints on the system.

The goal of each optimization analysis was to increase the elastic stiffness of the PHSS beam. A finite element model of a PHSS beam under four-point bending was developed and its maximum deflection was used to represent the change in stiffness. Consequently, the objective function of the optimization analysis was set to minimize the mid-span deflection with a stopping tolerance of 2% of the initial deflection.

The moment of inertia of a beam is dependent on its cross-sectional dimensions. These dimensions, which are the design variables, were varied in the optimization analysis and as a result the moment of inertia changed. The design variables which were used in the optimization analyses herein are:

$$[1] \quad 2*b_1 + b_2 \leq b$$

$$[2] \quad 2*b_3 + 2*b_4 + b_5 \leq b$$

$$[3] \quad h_1 + h_2 + h_3 + h_4 \leq h.$$

The original values of the design variables  $b_1$ ,  $b_2$ ,  $b_3$ ,  $b_4$ ,  $b_5$ ,  $h_1$ ,  $h_2$ ,  $h_3$ ,  $h_4$  are provided in Table 2. The values of  $b$  (overall PHSS width) and  $h$  (overall PHSS depth) are constant and their values are provided in Table 2. The original PHSS thickness  $t$  is also given in Table 2. It is constant for some of the optimization analyses, while in others it was permitted to vary.

Furthermore, a state variable that constrained the FE models within acceptable design limits was implemented. The state variable herein was the cross-sectional area of the PHSS which was either kept constant or allowed to increase up to 20% of the original. Finally, for each optimization analysis, the mesh size was kept constant, and only hexahedral elements were used.

The design optimization was completed via the first order analysis method (Huebner et al., 2001). This method is an iterative procedure, and the steps involved are described below:

1. Start with an initial design or cross-section  $x^0$ . Set the iteration counter  $k = 0$ .
2. Calculate the displacement or deflection vector  $u(x^k)$  for the current design by performing a finite element (FE) analysis:  $K(x)u(x) = F(x)$ , where  $K$  and  $F$  are the stiffness and force vectors, respectively.
3. For the current design or cross-section  $x^k$ , calculate the objective function, the constraint functions and determine their gradient,  $\nabla g(x^k)$ . For optimization problems, the local (global) minima are located at points for which the gradient is zero.
4. For each  $x^k$  formulate an explicit, convex approximation  $S^k$  for the problem.
5. Solve  $S^k$  via an optimization algorithm such as the Taylor Series to give a new design or cross-section  $x^{k+1}$ .
6. Put  $k = k+1$  and return to step ii) unless a stopping criterion or tolerance is satisfied.

### 2.1 Verification of the Finite Element Model

In order to accurately complete the optimization study, the FE model of the PHSS beam was initially verified. The verification process involved comparing the numerical deflection at the mid-point of the beam to the corresponding theoretical deflection.

The numerical analyses were conducted up to load  $P$  of 200 kN. This load was determined from the experimental tests as the elastic region limit for the test specimen, Figure 3. The beams analysed were made of cold-formed steel ( $E_s = 200,000$  MPa), 3658 mm in length. The moment of inertia was varied during the optimization analysis as the cross-sectional dimensions changed. The beam supports and loading points consisted of profiled plates to match the

shape of the PHSS, as shown in Figure 4, with a width of 152 mm to ensure adequate bearing resistance. The loading points were 1000 mm apart ( $L_2$ ).

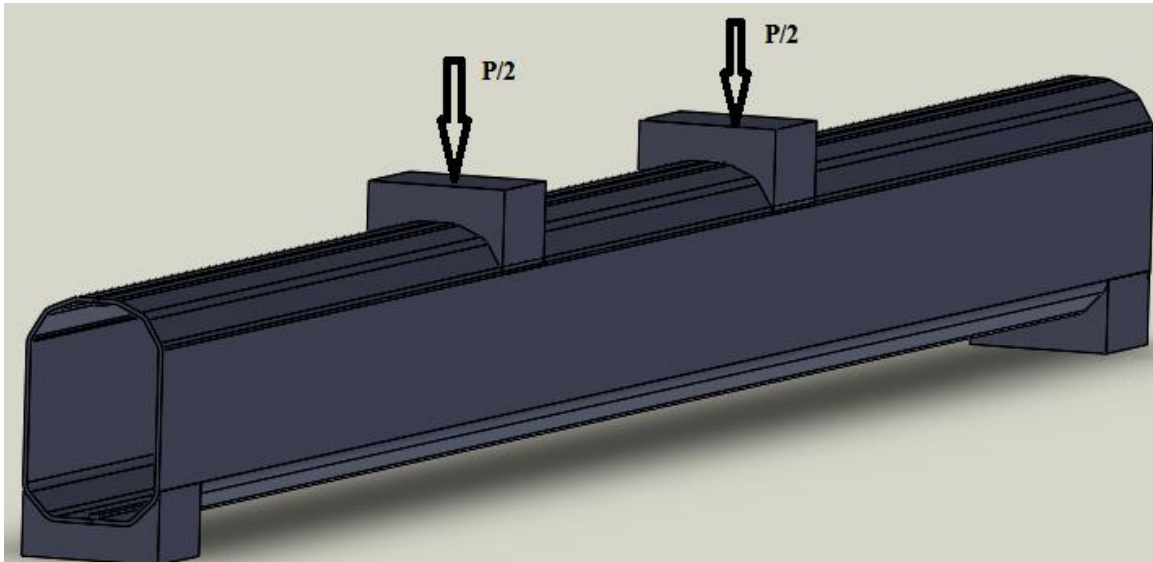


Figure 4: 3-D FE model of the proposed PHSS

The FE model of the proposed PHSS beam was built using hexahedral Solid185 brick elements in ANSYS APDL 15.0, and all the design variables were defined parametrically. The bottom-up meshing technique was used for the 3-D model. The mesh size (1 mm x 1 mm), which controlled the number of brick elements, was dependent on the available computing power, and the required level of accuracy.

The distance between the support points ( $L$ ) was 3500 mm, and each of the point loads was 1250 mm ( $L_1$ ) from the support points. The initial cross-sectional dimensions of the FE model are shown in Table 2.

Based on the initial design variables, a FE model with 50,656 Solid185 brick elements and a load  $P$  of 200 kN, the mid-point deflection of the proposed PHSS beam was determined to be 10.53 mm, with a moment of inertia of  $69.3 \cdot 10^6 \text{ mm}^4$ . On the other hand, the theoretical equation for the maximum deflection at the mid-point of a beam in four-point bending with this moment of inertia predicted 11.4 mm. The obtained numerical and theoretical solutions differ by only 7.6%, which was deemed to be reasonable agreement. This discrepancy is likely due to differences in loading (point loads versus loading through plates in the finite element model) and support conditions (true pin and roller supports versus plate supports in the finite element model).

## 2.2 Design Optimization

In order to investigate the effect of the cross-section shape on the elastic stiffness of a PHSS beam, three optimization analyses were conducted.

The first analysis investigated how close the original cross-section was to an “optimized” shape in terms of elastic stiffness. Only the vertical dimensions of the webs,  $y_4$  and  $y_5$ , were permitted to vary. The updated cross-section was constrained to have the same plate thickness,  $t$ , and cross-sectional area, as the original.

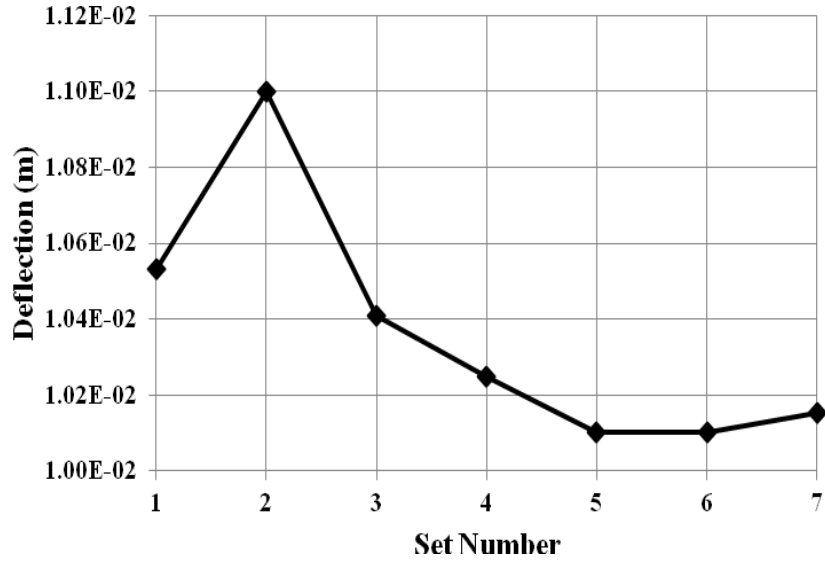


Figure 5: Deflection vs design sets for the first optimization analysis

Figure 5 shows the maximum midpoint deflections of the PHSS beam as the design variables were changed. Each specific set of new design variables is termed a “Set Number” with Set 1 representing the original cross-section. The minimum deflection was obtained for the Set 5 parameters. Figure 6 shows the cross-section corresponding to Set 5, and, for comparison, the original cross-section. The Set 5 dimensions are also listed in Table 3.

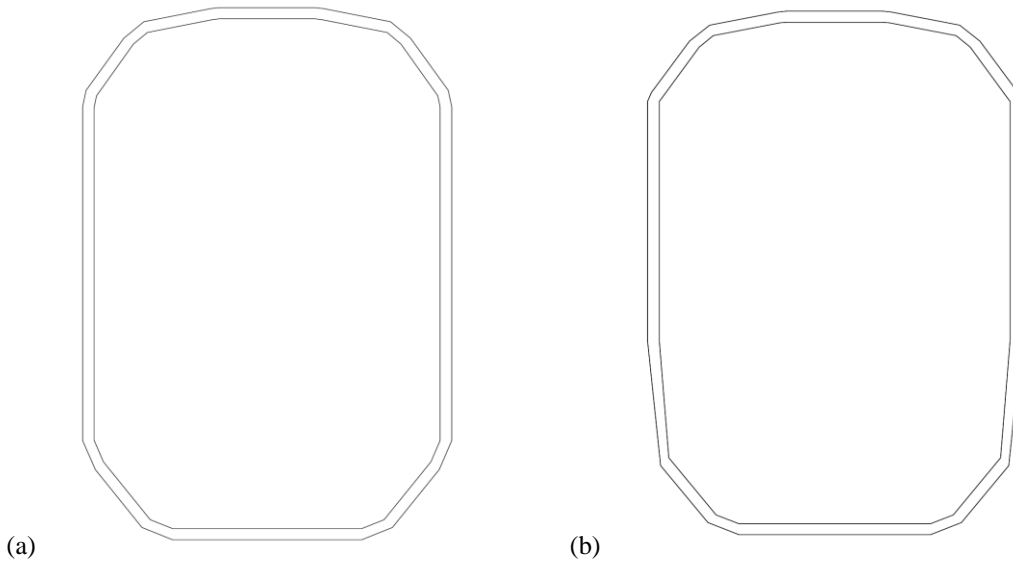


Figure 6: Comparison of the original cross-section (a), and the Set 5 cross-section (b)

Table 3: Dimensions of the different cross-sections of the PHSS beam

Design Variable	Set 5 Length (mm)	Set 7 Length (mm)	Set 4 Length (mm)
b	203	203	203
b <sub>1</sub>	49.5	41.55	49.6
b <sub>2</sub>	104	119.9	103.8
b <sub>3</sub>	33.5	28.6	34.8
b <sub>4</sub>	42	46.3	40.7
b <sub>5</sub>	52	53.2	52
h	305	305	305
h <sub>1</sub>	112.5	79.8	61.3
h <sub>2</sub>	140	169.8	186.3
h <sub>3</sub>	35.1	47.3	49.3
h <sub>4</sub>	17.4	8.1	8.1
t	6.4	N/A	N/A

In the first analysis, the optimized cross-section has a 4.3% higher flexural stiffness as compared to the original. This increase was obtained by significantly reducing the height of the web  $h_2$  by 26.7% (Table 3). It is possible that the slender web dimension  $h_2$  in the original cross-section leads to ovalization of the PHSS beam during bending, which lowers its stiffness (Guarracino, 2003). Therefore, by reducing  $h_2$  in Set 5 the flexural stiffness is increased. This increase, however, is quite modest, suggesting the original cross-section was already close to “optimum” in terms of flexural stiffness.

In the second optimization, all the constraints, including the thickness, were relaxed somewhat with the overall cross-sectional area permitted to increase up to 20% of the original. The cross-sectional dimensions in Set 5, Set 6, and Set 7 provided the lowest deflections, Figure 7. However, the cross-sectional areas for Set 5 and Set 6 exceeded the area of the original by more than 20%. Thus Set 7 was chosen as the optimum solution.

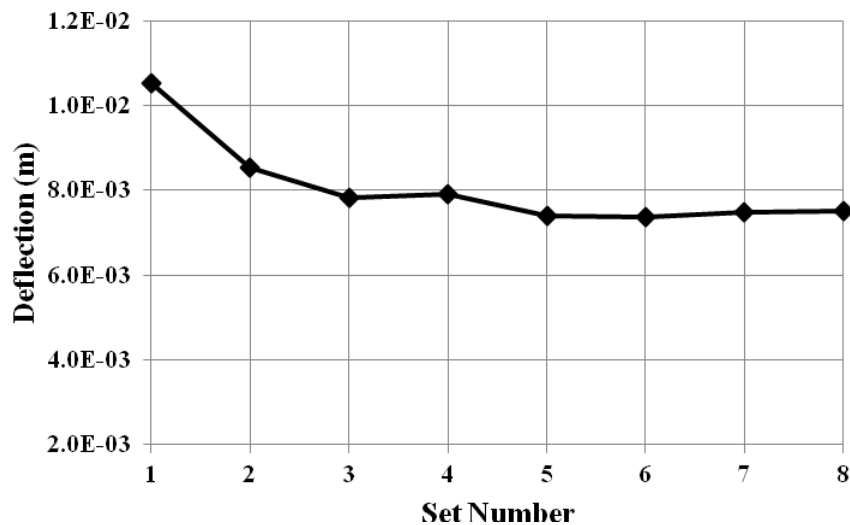


Figure 7: Deflection vs design sets for the second optimization analysis

The Set 7 cross-section, whose dimensions are shown in Table 3, increased the stiffness of the PHSS beam by 40.5%. As would be expected, the flexural stiffness can be increased with more area located away from the centroid, and this optimized cross-section significantly increased the area of its top and bottom flanges by 19.6%, Figure 9(a).

With the final optimization analysis, all the design variables,  $b_1$ ,  $b_2$ ,  $b_3$ ,  $b_4$ ,  $b_5$ ,  $h_1$ ,  $h_2$ ,  $h_3$ ,  $h_4$ , and  $t$  were allowed to change. However, the total cross-sectional area was kept constant in relation to the original cross-section.

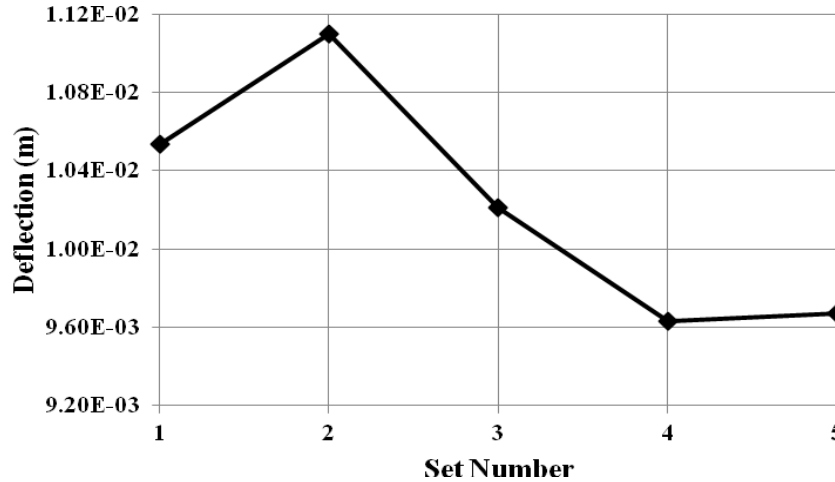


Figure 8: Deflection vs design sets for the final optimization analysis

In the final optimization analysis, the cross-sectional dimensions of Set 4 resulted in the lowest deflection. This cross-section, Figure 9(b), increased the stiffness of the PHSS beam by 9.4% with no increase in the overall area.

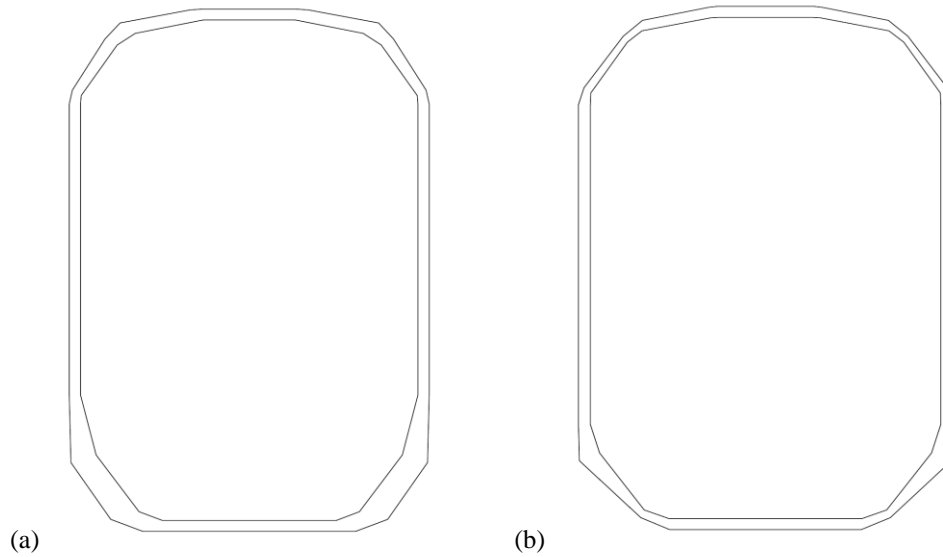


Figure 9: Illustration of the cross-sections from Set 7 (a), and Set 4 (b)

The reduction of the deflection of the PHSS beam was achieved by reducing the height  $h_2$  of its web (Table 3) while redistributing more of its cross-sectional area to the tension flange, as shown in Figure 9(b). This helped minimize ovalization during bending, and consequently increased the stiffness of the PHSS beam. Note that both of the optimized sections in Figure 9 have variable wall thicknesses. This certainly would make fabrication more costly; however these sections could be obtained through steel castings (Baddoo, 1996).



### 3. CONCLUSION

An optimization algorithm proposed by Huebner et al., 2001 has been adopted in this paper to investigate the bending stiffness of polygonal hollow structural sections. An elastic finite element model using a commercial package was used to predict the deflections of a PHSS subjected to 4-point bending. The following conclusions were drawn from this work:

1. The numerical optimization process is feasible. Solutions were found to typically converge in 5 iterations. The design optimization method and FE analyses offer an inexpensive method of optimizing the cross-section of structural sections compared to experimental testing.
2. Constraining the algorithm so that no increase in cross-sectional area is permitted, an optimized PHSS was obtained that had a 9.4% higher bending stiffness compared to the original section.
3. Allowing the algorithm to increase the total cross-sectional area, an optimized PHSS was obtained that had a 40.5% higher bending stiffness, with only a 19.6% increase in area, compared to the original section.
4. Both optimized sections have a variable wall thickness, which may not be the most economical from a fabrication perspective. In such instances, steel castings would have to be used.

### ACKNOWLEDGEMENTS

The authors would like to thank the Natural Sciences and Engineering Research Council of Canada (NSERC), Queen's University, and Ankor Engineering Ltd. for all the support they provided. The authors also appreciate the contributions of Dr. Il Yong Kim and Jon Wong.

### REFERENCES

- Yamashita, M., Gotoh, M., and Sawairi, Y. 2003, Axial Crush of Hollow Cylindrical Structures with Various Polygonal Cross-sections Numerical Simulation and Experiment, Department of Mechanical and Systems Engineering, Gifu University, Japan. *Journal of Materials Processing Engineering*, 59-64.
- Huebner, K.H., Dewhurst, D.L., Smith, D.E., and Byrom, T.G. 2001, *The Finite Element Method for Engineers*, New York, NY, USA, pg.570-636.
- F. Guarracino. 2003, On the Analysis of Cylindrical Tubes Under Flexural: Theoretical Formulation, Experimental Data and Finite Element Analyses, Department of Civil Engineering, University of Napoli. *Thin Walled Structures*, 127-147.
- Theofanous, M., Chan, T. M. and Gardner, L. 2009, Structural Response of Stainless Steel Oval Hollow Section Compression Members. *Engineering Structures*, 31, 922-934.
- Gardner L, Ministro A. 2004, Testing and numerical modelling of structural steel elliptical and oval hollow sections, London, Department of Civil and Environmental Engineering. *Imperial College of London*, 04-002-ST.
- Baddoo, N.R.. 1996, *Castings in Construction*, The Steel Construction Institute, Silwood Park, Ascot, Berkshire, SL5 7QN, SCI Publication 172.